

**NIST Internal Report  
NIST IR 8468**

**Laser tracker relative range error  
evaluation by the back-to-back,  
common path single pass, and  
common path double pass  
methods**

Marcos Motta de Souza  
Bala Muralikrishnan  
Vincent Lee  
Daniel Sawyer

This publication is available free of charge from:  
<https://doi.org/10.6028/NIST.IR.8468>

NIST Internal Report  
NIST IR 8468

# Laser tracker relative range error evaluation by the back-to-back, common path single pass, and common path double pass methods

Marcos Motta de Souza  
*National Institute of Metrology,  
Quality and Technology (INMETRO),  
Rio de Janeiro, 25250020, Brazil*

*Sensor Science Division  
Physical Measurement Laboratory  
National Institute of Standards and  
Technology,  
Gaithersburg, MD 20899, USA*

Bala Muralikrishnan  
Vincent Lee  
Daniel Sawyer  
*Sensor Science Division  
Physical Measurement Laboratory  
National Institute of Standards and  
Technology,  
Gaithersburg, MD 20899, USA*

This publication is available free of charge from:  
<https://doi.org/10.6028/NIST.IR.8468>

August 2023



U.S. Department of Commerce  
*Gina M. Raimondo, Secretary*

National Institute of Standards and Technology  
*Laurie E. Locascio, NIST Director and Under Secretary of Commerce for Standards and Technology*

NIST IR NIST IR 8468  
August 2023

Certain commercial equipment, instruments, software, or materials, commercial or non-commercial, are identified in this paper in order to specify the experimental procedure adequately. Such identification does not imply recommendation or endorsement of any product or service by NIST, nor does it imply that the materials or equipment identified are necessarily the best available for the purpose.

### **NIST Technical Series Policies**

[Copyright, Use, and Licensing Statements](#)

[NIST Technical Series Publication Identifier Syntax](#)

### **Publication History**

Approved by the NIST Editorial Review Board on 2023-05-24

### **How to Cite this NIST Technical Series Publication**

Motta de Souza M, Muralikrishnan B, Lee V, Sawyer D (2023) Laser tracker relative range error evaluation by the back-to-back, common path single pass, and common path double pass methods. (National Institute of Standards and Technology, Gaithersburg, MD), NIST Internal Report (IR) NIST IR 8468.  
<https://doi.org/10.6028/NIST.IR.8468>

### **NIST Author ORCID iDs**

Marcos Motta de Souza: 0009-0006-0564-902X

Bala Muralikrishnan: 0000-0002-0313-9708

Vincent Lee: 0000-0002-2953-6322

Daniel Sawyer: 0009-0009-2407-6708

### **Contact Information**

[mmsouza@inmetro.gov.br](mailto:mmsouza@inmetro.gov.br)

[bala.muralikrishnan@nist.gov](mailto:bala.muralikrishnan@nist.gov)

[vincent.d.lee@nist.gov](mailto:vincent.d.lee@nist.gov)

[daniel.sawyer@nist.gov](mailto:daniel.sawyer@nist.gov)

## **Abstract**

The Dimensional Metrology Group (DMG) at the National Institute of Standards and Technology (NIST) has a unique 60 m long length facility that provides traceable reference lengths for the evaluation of measuring tapes, optical fibers, electronic distance meters, laser trackers and terrestrial laser scanners. In this report, we compare three methods to evaluate the ranging error of laser trackers in this facility. These include the back-to-back, the common path single pass, and the common path double pass method. We describe the different methods and compare them in terms of their advantages and disadvantages.

## **Keywords**

back-to-back; common path; double pass; laser tracker; maximum permissible error; relative range error; single pass, test uncertainty.

## Table of Contents

<b>1. Introduction</b> .....	<b>1</b>
<b>2. Back-to-back method</b> .....	<b>1</b>
2.1. Test setup.....	1
2.2. Measurement sequence .....	2
2.3. Results.....	4
2.4. MPE.....	4
2.5. Test uncertainty .....	5
2.5.1. Interferometer zeroed near the beam splitter.....	5
2.5.2. Interferometer zeroed near the laser tracker.....	6
2.6. Discussion .....	8
<b>3. Common path single pass method</b> .....	<b>8</b>
3.1. Test setup.....	8
3.2. Measurement sequence .....	9
3.3. Results.....	10
3.4. MPE.....	11
3.5. Test uncertainty .....	11
3.6. Discussion .....	11
<b>4. Common path double pass method</b> .....	<b>11</b>
4.1. Test setup.....	11
4.2. Measurement sequence .....	14
4.3. Results.....	14
4.4. MPE.....	15
4.5. Test uncertainty .....	15
4.6. Discussion .....	16
<b>5. Conclusions</b> .....	<b>16</b>
<b>References</b> .....	<b>17</b>

## **Acknowledgments**

We thank Matthias Saure at Leica Geosystems for detailed responses to our questions. We thank the International and Academic Affairs Office (IAAO) at NIST for funding the first author's visit to NIST through the NIST-SIM Engagement Opportunity program. We are especially grateful to Andrew Conn at the IAAO for his support. We also thank Patrick Egan, Braden Czapla, and Daniel Adler at NIST for reviewing the document.

## 1. Introduction

The tape tunnel laboratory in the Dimensional Metrology Group (DMG) at the National Institute of Standards and Technology (NIST) is a unique facility in the United States. The facility provides traceable long reference lengths that allows for the calibration of measuring tapes, optical fibers, electronic distance meters, laser trackers and terrestrial laser scanners. It houses a 60 m long rail with a carriage. A stand-alone laser interferometer is mounted at one end of the rail and provides reference lengths traceable to the SI unit, the meter. The laboratory is temperature controlled to within  $\pm 0.1$  °C locally (i.e., at the location of a temperature sensor), with a maximum temperature difference of  $\pm 0.25$  °C over its full length at the height of the rail [1].

In this report, we describe the evaluation of the ranging unit of laser trackers in this tape tunnel facility. We consider errors and uncertainties in the laser interferometer's refractive index correction only. Errors in the dihedral angle of the interferometer retroreflector and lack of coincidence between the laser and tracker targets are not considered. We compare three methods to evaluate the ranging error – the back-to-back, common path single pass, and the common path double pass methods. One method may be chosen over the other based on space constraints and/or availability of equipment. We compare the three methods in terms of their advantages and disadvantages, in particular, their ability to evaluate the full range of the laser tracker and the ability to meet the ASME B89.4.19-2021 [2] requirement for measurement performance index ( $C_m$ ), which is the ratio of maximum permissible error (MPE) to expanded test uncertainty.

## 2. Back-to-back method

### 2.1. Test setup

In the back-to-back method, the instrument under test, i.e., the laser tracker, is placed at the one end of the tunnel while a stand-alone laser interferometer is placed at the other end [1] to provide reference values for displacements. The distance between them is about 62 m. The laser beams of the stand-alone interferometer and the laser tracker under test are aligned to be parallel along the length of the rail. A carriage with two reflectors is mounted as shown in Fig. 1. The reflector facing the laser tracker is a 1.5" spherically mounted retroreflector (SMR) while the one facing the stand-alone interferometer is a 4" cube corner reflector. Fig. 2 shows photos of the test setup.

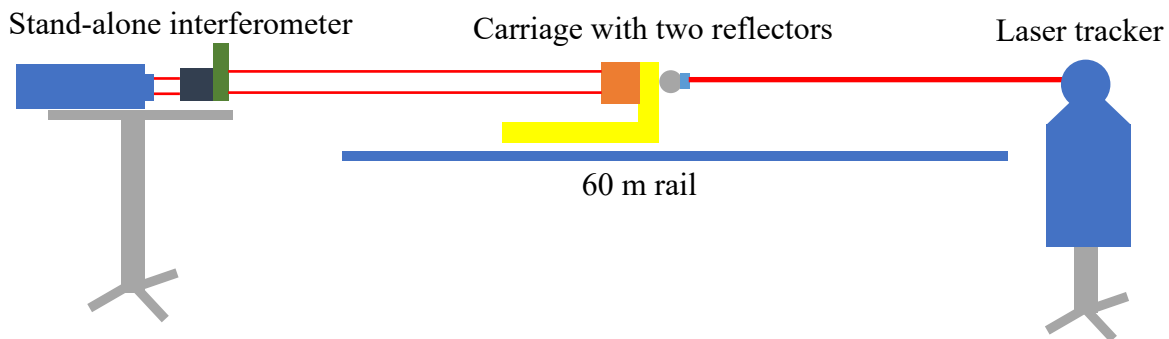


Fig. 1. Back-to-back test setup.



**Fig. 2.** (a) Stand-alone interferometer and the carriage at one end of the tape tunnel, (b) the tracker under test at the other end of the tape tunnel, (c) the carriage with two reflectors, one for the tracker under test and one for the stand-alone interferometer.

## 2.2. Measurement sequence

We explain the measurement sequence with the aid of Fig. 3. In the figure, all distances  $r$  are with respect to the beam splitter of the stand-alone interferometer (to facilitate later discussion on deadpath). The carriage is initially brought to a distance of  $r_0 \sim 0.2$  m from the beam splitter of



the stand-alone interferometer, so that the laser tracker reads a range of about 61.8 m. The interferometer is zeroed at this location of the carriage (subscript 0 indicates that interferometer is zeroed here). For the measurements, we consider seven positions of the carriage (distances of  $r_0$  through  $r_6$  from the beam splitter), each about 10 m from the previous location, as shown in Fig. 3. The measurement sequence begins by moving the carriage to the position closest to the laser tracker, i.e., a distance of  $r_6 = 60.2$  m from the beam splitter, so that the laser tracker reads a range of 1.8 m. All displacement calculations are performed with respect to this position. Both the stand-alone interferometer and the laser tracker perform a measurement at this position ( $r_6$ ). The carriage is then moved to the next position ( $r_5$ ) and both instruments perform a measurement. This process is repeated for all seven positions ( $r_6$  to  $r_0$ ) over this run. The carriage is then brought back to the starting position ( $r_6$ ) and the entire process repeated for a total of five runs of measurements. The laser beam of the laser tracker is never broken during this sequence, thus the entire measurement is performed in the InterFeroMeter (IFM) mode of the laser tracker. Another set of five runs are then performed to test the absolute distance meter (ADM) of the laser tracker. During this set of five runs, the laser beam of the laser tracker is always broken prior to acquiring data, thus the entire measurement is performed in the ADM mode.

Note that the quantities of interest, the relative range errors, are the difference in displacements seen by both instruments, calculated with respect to the position that is closest to the laser tracker, which is the starting position ( $r_6$ ). For example, as the carriage is moved from  $r_6$  to  $r_1$ , both instruments record the displacement ( $d_{16}$ ), and the relative range error is calculated for position  $r_1$ . This is done for all positions  $r_i$ ,  $i = 0$  to 6 (displacements are always calculated with respect to  $r_6$ ). These relative range errors are presented in the next Section.

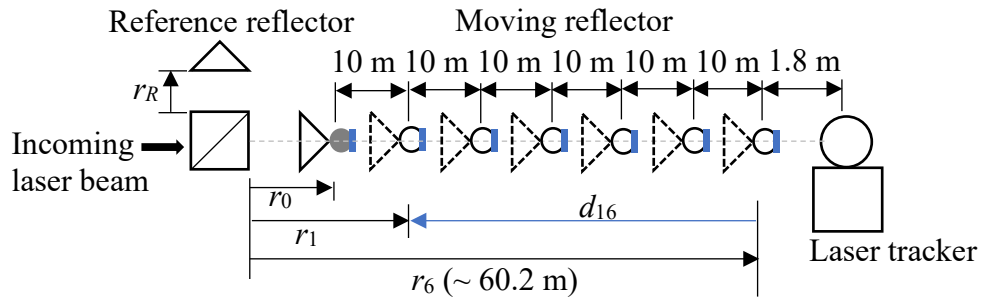


**Fig. 3.** Seven positions of the carriage (shown only by the cube corner and SMR) along with the location of the stand-alone interferometer and the laser tracker are shown. An example of the quantity of interest,  $d_{16}$ , is also shown.

The displacement  $d_{i6}$  (for  $i = 0$  through 6, and second subscript, 6, indicates displacements are with respect to position 6) seen by the stand-alone interferometer when the carriage is moved from the starting position ( $r_6$ ) to any other position (say,  $r_5$ ) is given by

$$d_{i6} = r_{60} + c_6 - (r_{i0} + c_i), \quad (1)$$

where

$$r_{i0} = r_i - r_0, \quad i = 0 \text{ to } 6, \quad (2)$$

and  $c$  is the deadpath correction (see Stone and Phillips [3] for a detailed discussion on the effect of deadpath). Specifically,  $c_6$  is the deadpath correction for the displacement  $r_{60}$  ( $= r_6 - r_0$ ) and more generally, for any value of  $i$  from 0 to 6,  $c_i$  is the deadpath correction for the displacement  $r_{i0}$  ( $= r_i - r_0$ ). Deadpath is the difference in optical path length between the measurement and reference arms at the beginning of the measurement when the interferometer is set to zero. The correction  $c_i$  given by

$$c_i = (r_0 - r_R) \frac{\Delta\lambda}{\lambda_0}. \quad (3)$$

In Eq. (3),  $\lambda_0$  is the wavelength when the interferometer is zeroed (at the  $r_0$  location),  $\Delta\lambda$ , is the difference in wavelength of the beam along the deadpath, between the measurements at the two positions ( $r_i$  and  $r_0$ ), and  $r_R$  is the distance to the reference cube corner as shown in Fig. 3. When the interferometer is zeroed near the beam splitter,  $c$  is negligibly small (because  $r_0 - r_R \sim 0$ ), and its effect can be ignored. However, if the interferometer is zeroed when the carriage is near the laser tracker ( $r_6$ ), the dead path will be extremely large, about 60 m. We will discuss this situation in Section 2.5.

### 2.3. Results

Fig. 4(a) shows the relative range errors from five runs of the IFM of the tracker under test. The data shows linear errors of approximately  $0.4 \mu\text{m}/\text{m}$  ( $25 \mu\text{m}$  over 60 m). The temperature sensor of the tracker under test was reading  $0.1 \text{ }^\circ\text{C}$  larger than the average temperature along the beam path while the pressure sensor was reading about 66.66 Pa (0.5 mm Hg) lower than the reference value. Both deviations are within manufacturer specifications for the weather station. Note that the laser tracker only samples temperature at one location along the beam path. We choose this location to be as close as possible to one of the seven temperature sensors that was reporting temperature within  $\pm 0.02 \text{ }^\circ\text{C}$  of the average temperature along the beam path. The error in the measured length due to temperature is about  $0.1 \mu\text{m}/\text{m}$ , while the error due to pressure is about  $0.2 \mu\text{m}/\text{m}$ , for a total of about  $0.3 \mu\text{m}/\text{m}$ . Thus, a significant portion of the observed length error is due to the errors in the weather station of the tracker under test. Fig. 4(b) shows the relative range errors from five runs of the ADM. As before, a significant portion of the linear errors are due to the weather station of the tracker under test.

### 2.4. MPE

The MPE for the IFM is listed as  $0.5 \mu\text{m}/\text{m}$  in the specification sheet [4] provided by the manufacturer of the laser tracker. Clarifications provided by manufacturer indicate that this specification only accounts for errors in the temperature sensor, not the pressure sensor. Adding another  $0.3 \mu\text{m}/\text{m}$  due to the pressure sensor [5], the MPE is given by  $0.8 \mu\text{m}/\text{m}$ , thus for a displacement of 60 m, the MPE is  $48 \mu\text{m}$ .

Again, based on clarifications provided by the manufacturer of the laser tracker, the MPE for the ADM is calculated as  $\sqrt{(10 + 0.8(d + 1.8))^2 + (10 + 0.8 * 1.8)^2}$  for displacements of  $d$  starting from the 1.8 m position of the laser tracker. The factor of  $10 \mu\text{m}$  is the term associated with the dynamic lock-on accuracy of the ADM, a quantity provided by the manufacturer in their specifications. The MPEs are shown in Figs. 4(a) and (b). Note that we only show the positive

MPE line in all plots in this report because the measured errors are positive. MPEs limits extend in the negative direction as well.

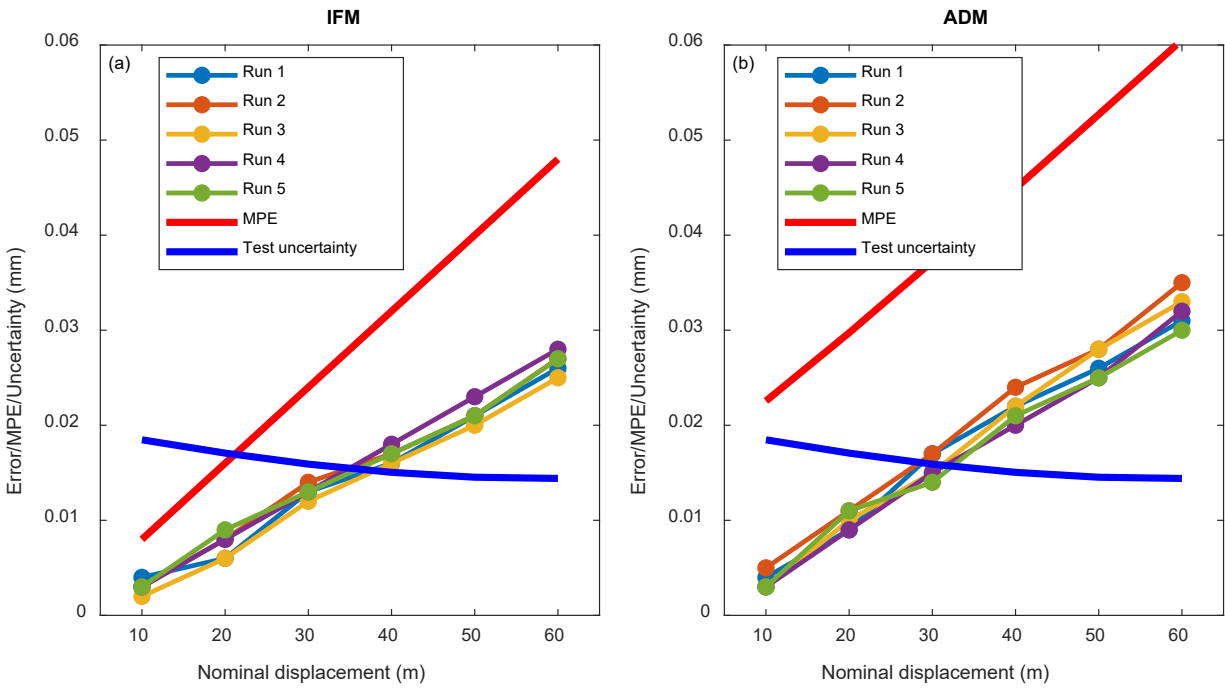


**Fig. 4.** Relative range errors, MPE, and expanded test uncertainty ( $k = 2$ ) for the back-to-back case when the stand-alone interferometer is zeroed near the beam splitter for the (a) IFM of the laser tracker under test, (b) ADM of the laser tracker under test. Nominal displacement is referenced to the tracker zero.

## 2.5. Test uncertainty

### 2.5.1. Interferometer zeroed near the beam splitter

As mentioned in Section 2.2, the displacement  $d_{i6}$  is given by

$$d_{i6} = r_{60} + c_6 - (r_{i0} + c_i) \quad (4)$$

The dominant contributor to the uncertainty in the displacement  $r_{i0}$  is due to uncertainty in the average temperature along the beam path. Air temperature along the laser beam path is measured using an array of seven calibrated thermistors. The standard uncertainty following NIST calibration is  $0.01 \text{ }^\circ\text{C}$  for each thermistor. However, there are spatial gradients along the rail, estimated to be  $\pm 0.25 \text{ }^\circ\text{C}$ . Assigning a uniform distribution to the average temperature then yields a standard uncertainty of  $0.12 \text{ }^\circ\text{C}$ . This results in a standard uncertainty in the reference displacement ( $r_{i0} = r_i - r_0$ ) measurement in the tape tunnel facility of  $0.12 \text{ } \mu\text{m/m}$  [1, 6]. As mentioned in Section 2.2, because the stand-alone interferometer is zeroed near the beam splitter, there is negligible deadpath in the measurements and its uncertainty is also negligible.

The uncertainties in  $r_{i0}$  (primarily due to uncertainty in the average temperature along the beam path) are given by

$$u_{r_{60}} = 0.12(r_6 - r_0) = 0.12 \times 60 = 7.2 \text{ } \mu\text{m}, \quad (5)$$

and

$$u_{r_{i0}} = 0.12(r_i - r_0) = 0.12 \times (60 - d_{i6}). \quad (6)$$

The test uncertainty, which is the uncertainty in the displacement, is then given by

$$u(d_{i6}) = \sqrt{u_{r_{60}}^2 + u_{r_{i0}}^2} = \sqrt{(0.12 \times 60)^2 + (0.12 \times (60 - d_{i6}))^2}. \quad (7)$$

The  $k = 2$  expanded test uncertainty is therefore

$$U(d_{i6}) = 2u(d_{i6}) = 2\sqrt{u_{r_{60}}^2 + u_{r_{i0}}^2} = 2\sqrt{(0.12 \times 60)^2 + (0.12 \times (60 - d_{i6}))^2}. \quad (8)$$

From Eq. (8) above, the expanded test uncertainty for a 10 m displacement is 18.8  $\mu\text{m}$  while the expanded test uncertainty for a 60 m displacement is 14.4  $\mu\text{m}$ . This uncertainty is larger for smaller displacements and smaller for larger displacements. The test uncertainties are also shown in Fig. 4. Note that the uncertainties are the same in Figs. 4 (a) and (b), only the MPEs are different.

### 2.5.2. Interferometer zeroed near the laser tracker

We now consider the case where the stand-alone interferometer is zeroed near the laser tracker (position  $r_0$ ), i.e.,  $r_0 - r_R = 60$  m as shown in Fig. 5. Then a correction  $c_i$  (in units of meters) given by

$$c_i = 60 \frac{\Delta\lambda}{\lambda_0} \quad (9)$$

has to be applied to the displacement recorded by the stand-alone interferometer. Although the nominal value of  $c_i$  is considered to be zero, there is an uncertainty associated with this correction, primarily due to uncertainty in temperature and pressure.

The uncertainty in average temperature in the beam path is 0.12  $^\circ\text{C}$  and the uncertainty in pressure is 10 Pa (0.075 mm Hg), resulting in uncertainty in wavelength of  $7.25 \times 10^{-5}$  nm and  $1.70 \times 10^{-5}$  nm, respectively, from Edlen's equation. Summing them in quadrature provides a wavelength uncertainty of  $7.45 \times 10^{-5}$  nm. The uncertainty in the deadpath correction is therefore given by

$$u_c = 60 \left( \frac{7.45 \times 10^{-5}}{633} \right) \times \sqrt{2} = 10 \text{ } \mu\text{m} \quad (10)$$

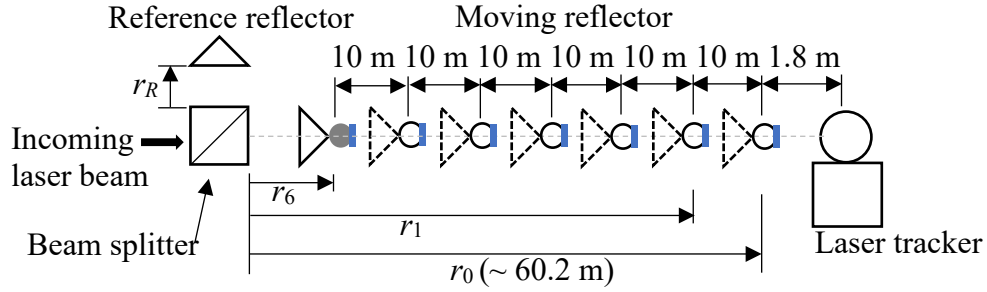


**Fig. 5.** Seven positions of the carriage along with the location of the stand-alone interferometer and the laser tracker.

The displacement  $d_{i0}$  (subscript 0 indicates displacements are with respect to the 0<sup>th</sup> position) seen by the stand-alone interferometer is given by

$$d_{i0} = r_{i0} + c_i, \quad (11)$$

where

$$r_{i0} = -(r_i - r_0), \quad i = 0 \text{ to } 6. \quad (12)$$

The test uncertainty, which is the uncertainty in the displacement, is given by the root sum squared of the deadpath uncertainty and the uncertainty due to temperature for a displacement  $r_{i0}$ , thus

$$u(d_{i0}) = \sqrt{u_c^2 + u_{r_{i0}}^2} = \sqrt{10^2 + (0.12d_{i0})^2}, \quad (13)$$

or

$$U(d_{i0}) = 2\sqrt{10^2 + (0.12d_{i0})^2}. \quad (14)$$

From Eq. (14) above, the expanded test uncertainty for a 10 m displacement is 20.1  $\mu\text{m}$  while the expanded test uncertainty for a 60 m displacement is 24.6  $\mu\text{m}$ . These uncertainties are larger than the uncertainties for the same displacements when we zero the stand-alone interferometer near the beam splitter.

Fig. 6 shows the test uncertainties for the two cases considered here – when the stand-alone interferometer is zeroed near the beam splitter (i.e, when laser tracker reads about 61.8 m) and when the stand-alone interferometer is zeroed near the laser tracker (i.e, when laser tracker reads about 1.8 m). Notice that the test uncertainty decreases with increasing displacement for the first case while it increases with increasing displacement for the second case.

## 2.6. Discussion

Fig. 4(a) shows that the test uncertainty is larger than the IFM MPE for up to about 20 m for the back-to-back method. The ASME B89.4.19-2021 requires that the MPEs be at least as large as the  $k = 2$  expanded test uncertainty, i.e., a measurement capability index  $C_m$  of 1 or larger. Thus, the back-to-back method is not a viable option for relative range error evaluation of IFMs for small displacements (if the laser tracker and stand-alone interferometer are separated by large distances). Fig. 4(b) shows that the test uncertainties are equal to or smaller than the MPEs, thus ADM testing is possible with this technique. In addition to the limitation that IFMs cannot be tested for small displacements, we are only able to test up to 60 m in our laboratory while the tracker under test has a maximum range of 80 m. While it is not a requirement in the ASME B89.4.19 that a laser tracker IFM be tested to its full range, a user may specify a full range test as part of the optional length test for ADMs as indicated in Table 6.4.1-1 in the ASME B89.4.19 standard, thus having the ability to test the full range is useful. Testing to full range might also reveal interesting characteristics near the end of the range, as we show in Sec 4.3.

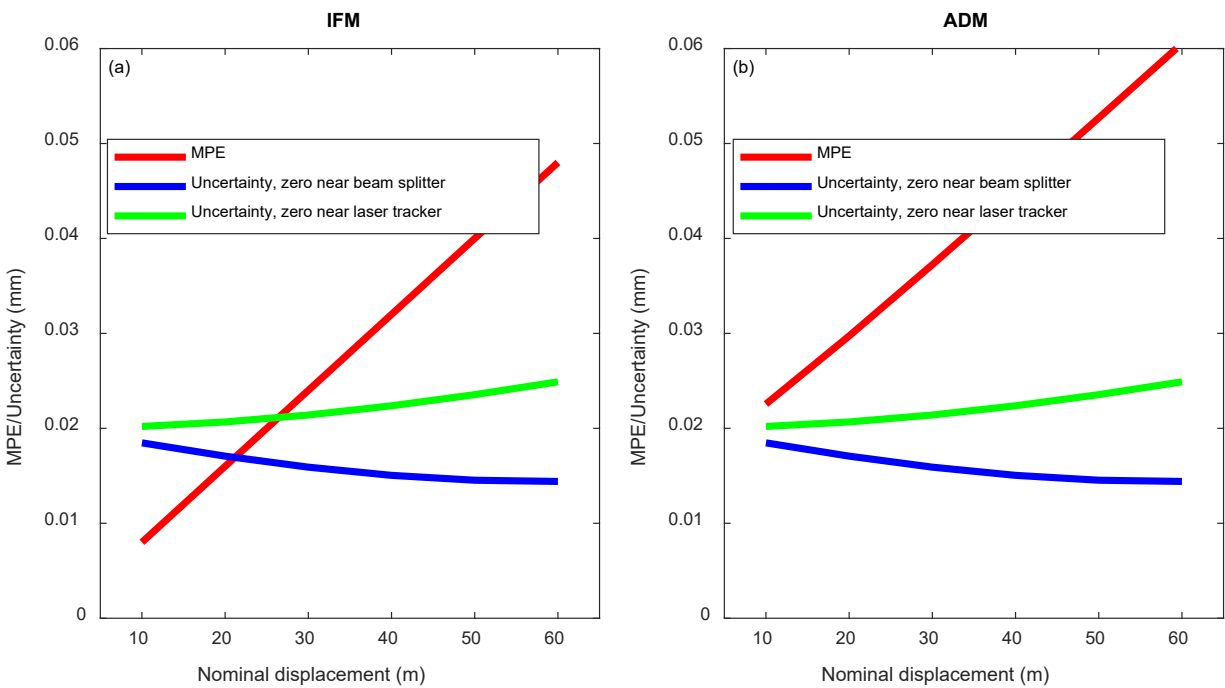


**Fig. 6.** MPE and  $k = 2$  expanded test uncertainties when the stand-alone interferometer is zeroed near the beam splitter versus near the laser tracker for the (a) IFM of the laser tracker under test, (b) ADM of the laser tracker under test. Note that the test uncertainties are the same for both plots, only MPEs are different. Nominal displacement is relative to the tracker zero.

## 3. Common path single pass method

### 3.1. Test setup

Because of the problems mentioned in the previous section regarding the large test uncertainty for small displacements, we switched to the common path single pass method in 2006 [7]. In this

method, the laser tracker and the stand-alone interferometer are near each other, i.e., at the same end of the tape tunnel. The outgoing and incoming laser beams of the stand-alone interferometer are separated using a periscope. A small fold mirror is placed between these beams so that the laser beam of the laser tracker under test bounces off this mirror, strikes the apex of the reflector, and returns to the laser tracker. Fig. 7 shows the schematic of this setup. Fig. 8 (a) and (b) shows photos of the setup. While we use a 4" SMR as the reflector on the carriage, a cube corner reflector is sufficient for the purpose.

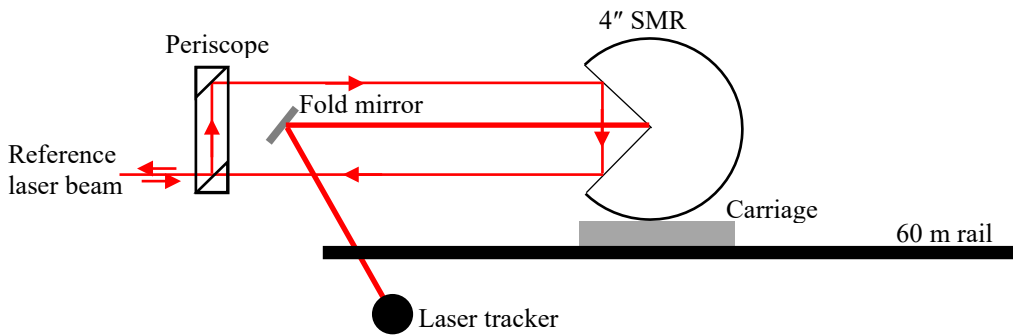


Fig. 7. Common path single pass test setup.

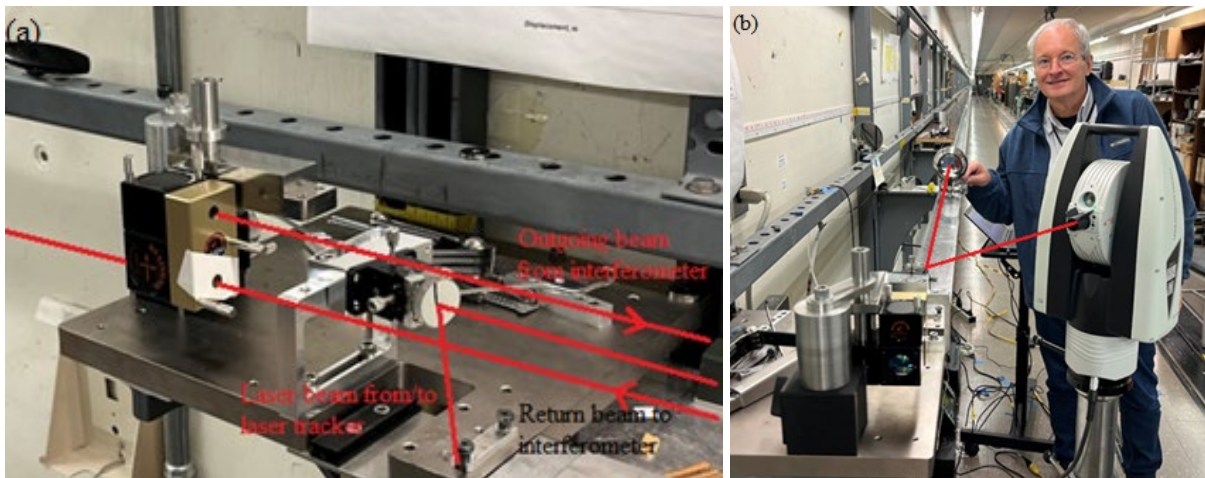


Fig. 8. (a) Showing the fold mirror placed between the outgoing and incoming reference laser beam, (b) showing the tracker under test placed near the fold mirror and the carriage with one reflector.

### 3.2. Measurement sequence

The measurement sequence begins by moving the carriage to the position closest to the laser tracker, i.e., a distance of  $r_0 = 0.2$  m from the beam splitter, so that the laser tracker reads a range of 1.5 m. The interferometer is zeroed at this location of the carriage. All displacement calculations are performed with respect to this position. We consider seven positions of the carriage as shown in Fig. 9. Both the stand-alone interferometer and the laser tracker perform a measurement at this position ( $r_0$ ). The carriage is then moved to the next position ( $r_1$ ) and both instruments perform a measurement. This process is repeated for all seven positions ( $r_0$  to  $r_6$ ).

over this run. The carriage is then brought back to the starting position ( $r_0$ ) and the entire process repeated for a total of five runs of measurements. The laser beam of the laser tracker is never broken during this sequence, thus the entire measurement is performed in the IFM mode of the laser tracker.

Another set of five runs are then performed to test the ADM of the laser tracker. During this set of five runs, the laser beam of the laser tracker is always broken prior to acquiring data, thus the entire measurement is performed in the ADM mode.

For the stand-alone interferometer, the displacement  $d_{i0}$  is given by

$$d_{i0} = r_{i0} + c.$$

where

$$r_{i0} = r_i - r_0 \quad i = 0 \text{ to } 6.$$

The deadpath correction,  $c$ , is negligibly small and its effect can be ignored.

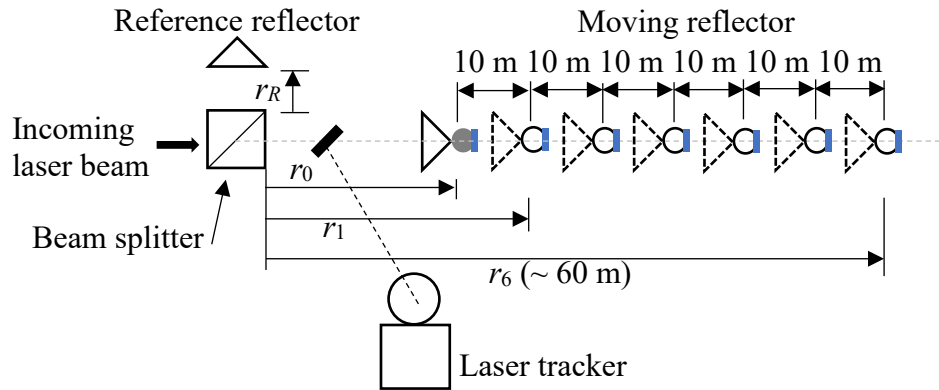


**Fig. 9.** Seven positions of the carriage (shown only by the cube corner and SMR) along with the location of the stand-alone interferometer and the laser tracker.

### 3.3. Results

Fig. 10(a) shows the relative range errors from five runs of the IFM of the tracker under test. Fig. 10(b) shows the relative range errors from five runs of the ADM of the tracker under test. As in the case of the back-to-back measurement, the weather station errors account for a significant portion of the linear errors seen in Fig. 10. The temperature sensor of the tracker under test was reading about 0.1 °C larger while the pressure sensor was reading about 40 Pa (0.3 mm Hg) lower, each contributing about 0.1 μm/m, for a total of 0.2 μm/m, i.e., 12 μm at 60 m.



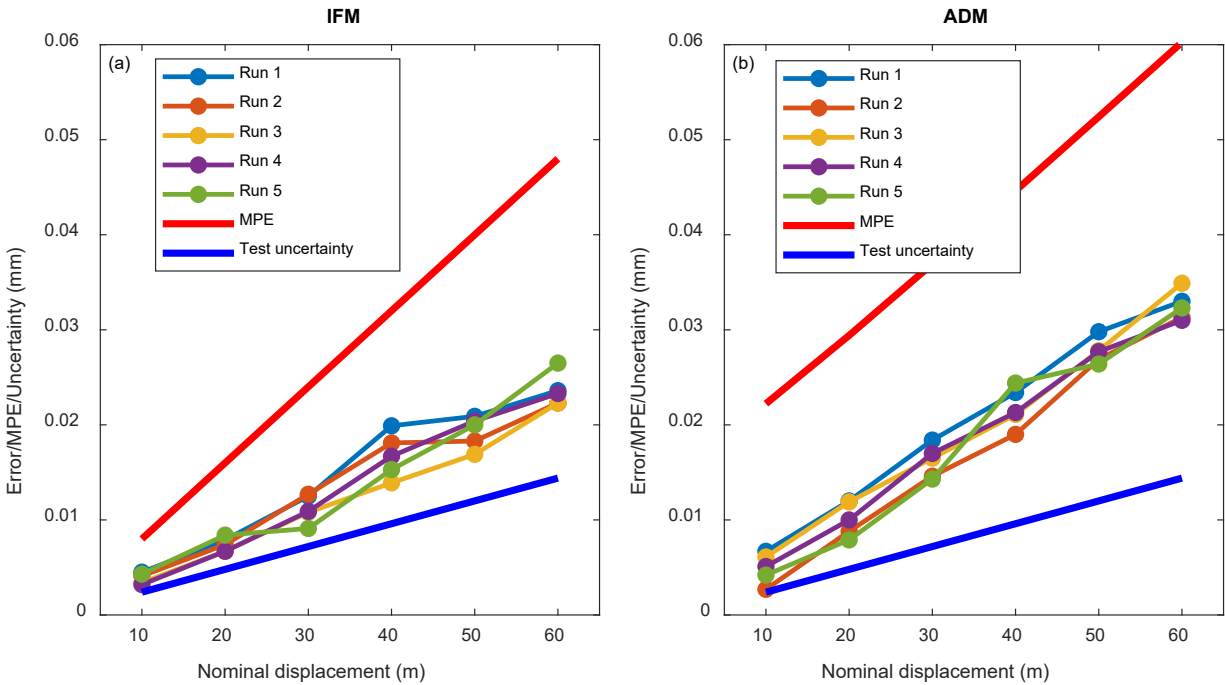


**Fig. 10.** Relative range errors, MPE, and test uncertainty for the common path single pass method for the (a) IFM of the tracker under test, (b) ADM of the tracker under test.

### 3.4. MPE

MPEs are calculated as described in Section 2.3 (and shown in Fig. 10) for the back-to-back method.

### 3.5. Test uncertainty

The test uncertainty is the uncertainty in the displacement  $r_i - r_0$ . This is given by  $0.12d_{i0}$ . The  $k = 2$  expanded test uncertainty is therefore  $0.24d_{i0}$ . These uncertainties are shown in Fig. 10. Because the laser beams of the laser tracker and the stand-alone interferometer travel a common path, the test uncertainty is proportional to displacement.

### 3.6. Discussion

While the common path single pass method overcomes one limitation of the back-to-back method, i.e., the problem of large test uncertainty for small displacements, the limitation of the maximum 60 m range remains for our facility.

## 4. Common path double pass method

### 4.1. Test setup

In order to measure the full range of the laser tracker, i.e., 80 m, we made a small modification to the common path single pass method based on work reported by Linville et al. [8]. We moved

the fold mirror slightly to one side and installed a spherically mounted retroreflector (SMR) next to it so that the laser beam of the laser tracker bounces off the fold mirror, strikes the 4" SMR on one face of the cube corner (instead of at its apex), strikes another face, and returns to lock onto the SMR as shown in Fig. 11. The outgoing and incoming laser beam from the stand-alone interferometer are displaced in the vertical plane while the outgoing and incoming laser beams of the laser tracker under test are displaced in the horizontal plane. When the carriage is moved by a certain amount, the laser tracker records twice the displacement seen by the reference. Thus, we can achieve 80 m displacement for the laser tracker using only a 40 m displacement of the carriage. Fig. 12 shows photos of the setup.

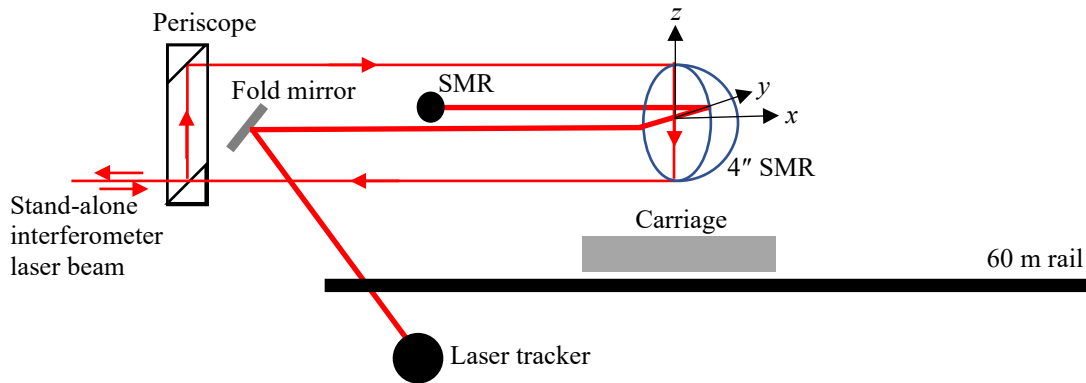


**Fig. 11.** Common mode double pass test setup.

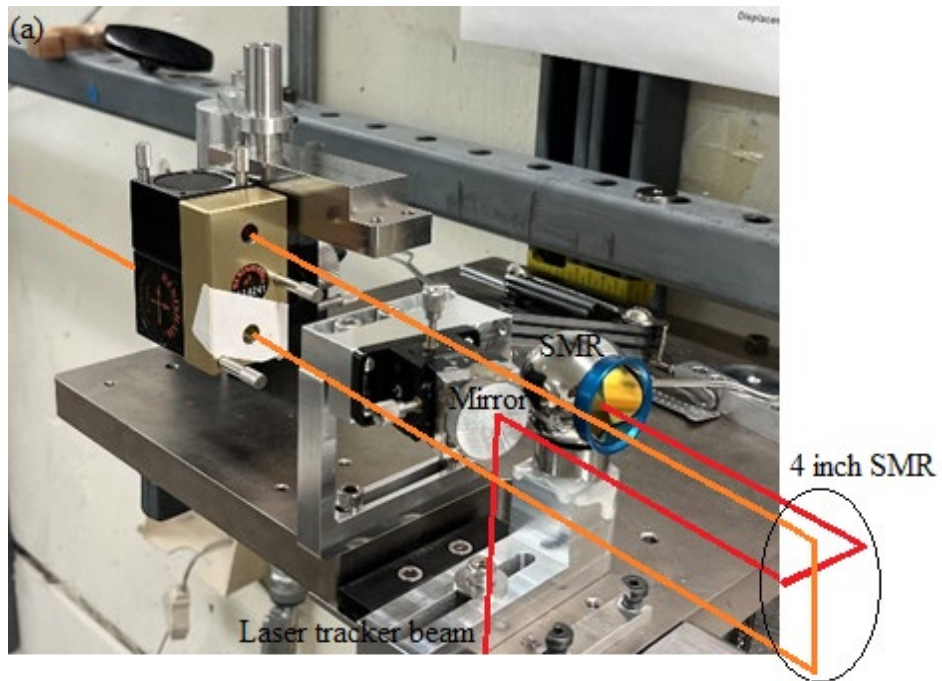


**Fig. 12.** (a) Fold mirror and SMR placed between the outgoing and incoming reference laser beam of the stand-alone interferometer and (b) the tracker under test placed near the fold mirror and the carriage with one reflector.

## 4.2. Measurement sequence

We consider nine positions of the carriage spaced 5 m apart from each other, i.e., the stand-alone interferometer records 5 m between positions. The laser tracker sees twice the amount, i.e., 10 m between positions. The overall measurement sequence is otherwise the same as described in Section 3.2.

## 4.3. Results

Fig. 13(a) shows the relative range errors from five runs of the IFM of the tracker under test. As before, the observed linear error is largely due to the errors in the weather station of the tracker under test. The pressure changed substantially between runs 2 and 3 but the weather station of the laser tracker did not capture the same change in pressure as the reference barometer, resulting in two clusters of data – runs 1 and 2 versus runs 3, 4, and 5.

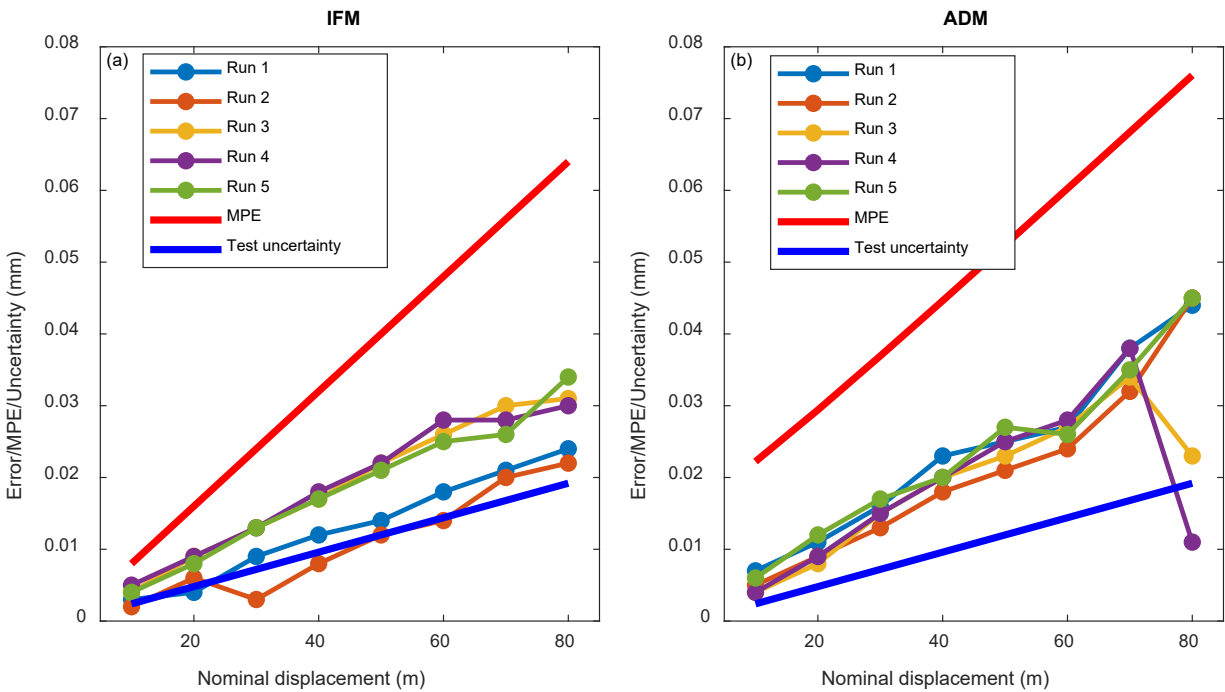


**Fig. 13.** Relative range errors, MPE, and test uncertainty for the common path double pass method for the (a) IFM of the tracker under test, (b) ADM of the tracker under test.

Fig. 13(b) shows the relative range errors from five runs of the ADM of the tracker under test. Notice the apparent lack of repeatability in the ADM data near the end of its range, 80 m. To investigate whether this lack of repeatability is random or systematic, we performed relative range error measurements over small increments of the carriage motion. We moved the carriage on the rail, so the laser tracker range was about 79600 mm. Without breaking the beam so the data is acquired in the IFM mode, we moved the carriage in steps of about 15 mm for a total travel of about 400 mm while recording both the laser tracker and stand-alone interferometer data (the interferometer was zeroed near the beam splitter). We then brought the carriage back to the starting point and acquired another set of data, but this time breaking the beam each time, so data is acquired in the ADM mode. The results are shown in Fig. 14(a). There is a periodic error

of large amplitude, about  $15\ \mu\text{m}$ , and a wavelength of about  $100\ \text{mm}$  for the ADM. Thus, depending on where the carriage is positioned, we can expect to see a relative range error for the ADM that is  $\pm 15\ \mu\text{m}$  of the average error at  $80\ \text{m}$ . This accounts for the apparent lack of repeatability in Fig. 13(b). The IFM does not exhibit this periodic error at  $80\ \text{m}$  as shown in Fig. 14(a). We repeated this experiment at the  $40\ \text{m}$  and  $60\ \text{m}$  distances for the ADM, see Fig. 14(b). No obvious periodic error is visible, although the data at  $60\ \text{m}$  is noisier than the data at  $40\ \text{m}$ .

We do note, however, that this periodic error was not reproducible in a subsequent repeat of this experiment. It is possible that this error was due to a disturbance in the polarization due to the multiple folding of the beam.

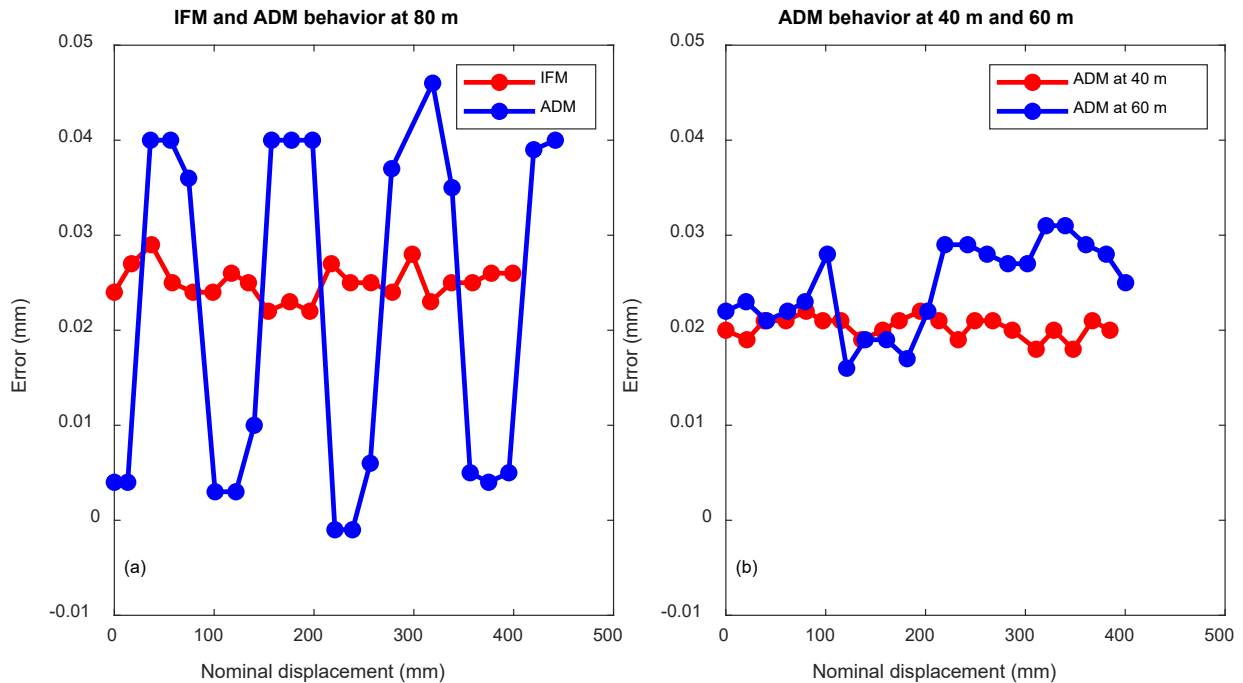


**Fig. 14.** (a) Relative range errors of the IFM and ADM at  $80\ \text{m}$ , zero on the x-axis corresponds to a distance of  $79600\ \text{mm}$  from the laser tracker (b) relative range errors of the ADM at  $40\ \text{m}$  and  $60\ \text{m}$ , zero on the x-axis corresponds to a distance of  $39600\ \text{mm}$  from the laser tracker for the red line (ADM at  $40\ \text{m}$ ) and a distance of  $59600\ \text{mm}$  for the blue line (ADM at  $60\ \text{m}$ ).

#### 4.4. MPE

MPEs are calculated as described in Section 3.3 (and shown in Fig. 13) for the back-to-back method.

#### 4.5. Test uncertainty

The  $k = 2$  expanded test uncertainty for a carriage displacement of  $d\ \text{m}$  is  $0.24d\ \mu\text{m}$ , as in the case of the common path single pass method. However, the laser tracker records a displacement that is twice the displacement seen by the stand-alone interferometer. Because the reference length  $d$  is doubled to obtain the reference for the laser tracker displacement, the uncertainty of

the error is  $2 \times 0.24d = 0.24L$ , where  $L$  is the displacement seen by the laser tracker. Thus, the  $k = 2$  expanded test uncertainty is still  $0.24 \mu\text{m/m}$  of laser tracker displacement, as in the case of the common path single pass method.

#### 4.6. Discussion

The common path double pass method allows the measurement of the full 80 m range of the tracker under test while also overcoming the problem of large test uncertainties for small displacements of the back-to-back method. Using a shorter portion of the tape tunnel also reduces the effect of thermal gradients along the beam path, thus producing more reliable estimates for the reference lengths. Measuring the full 80 m range of the ADM allowed us to observe periodic errors in the ADM at the 80 m range; this behavior was not evident at the 40 m or 60 m range.

#### 5. Conclusions

We described three methods to evaluate the relative range errors of a laser tracker in this report. The methods include the back-to-back, common path single pass, and the common path double pass. Table 1 summarizes the advantages and disadvantages of the methods.

**Table 1.** Comparison of different methods to evaluate laser tracker relative range error.

	<b>Advantages</b>	<b>Disadvantages</b>
Back-to-back	Easy to set up	Test uncertainties are not proportional to length, so cannot achieve $C_m$ ratio of greater than or equal to 1 for small displacements Cannot measure the full 80 m range of the tracker
Common path single pass	Test uncertainties are proportional to length, so small displacements have small uncertainties and large displacements have large uncertainties.	Relatively more difficult to setup, i.e., placing the fold mirror and aligning the laser beam of the laser tracker is more challenging than the back-to-back method. Cannot measure the full 80 m range of the tracker
Common path double pass	Can measure full 80 m range using only a 40 m rail Test uncertainties are proportional to length	Relatively more difficult to setup than the other two methods

## References

- [1] Estler WT, Sawyer DS, Borchardt B, Phillips SD (2006) Large-scale metrology instrument performance evaluation at NIST. *The Journal of the CMSC*, Autumn, 2006, pp 27-32.
- [2] ASME (2021) *ASME B89.4.19-2021: Performance Evaluation of Laser-Based Spherical Coordinate Measurement Systems* (ASME, New York, NY).
- [3] Stone J, Phillips SD, Mandolfo GA (1996) Corrections for wavelength variations in precision interferometric displacement measurements. *Journal of Research of the National Institute of Standards and Technology*, 101(5). <https://doi.org/10.6028%2Fjres.101.065>
- [4] Leica AT-960 laser tracker specification document. Available at <https://hexagon.com/products/leica-absolute-tracker-at960>, accessed on 2/15/2023.
- [5] Private communications with Matthias Saure at Leica Geosystems.
- [6] Ester WT (2006), Special tests of long-range displacement measurement performance, Draft technical procedure for laser tracker/radar range testing, 3/11/2006, *Internal document of the Dimensional Metrology Group, NIST*.
- [7] Blackburn C, Sawyer D, Shakarji C (2014) Common-path method for laser tracker ranging calibration. *The Journal of the CMSC*, 9(1), pp 4-7.
- [8] Linville DL, Park Y, Lin N, Lin Y (2019) Automated laser rail for ADM calibration. *Quality Digest*. Available at <https://www.qualitydigest.com/inside/cm-sc-article/automated-laser-rail-adm-calibration-052319.html>